Modelling of the adsorption of C-60 on the Au(110) surface

Baxter, RJ; Rudolf, P; Teobaldi, G; Zerbetto, F; Baxter, Richard J.

Published in:
Chemphyschem

DOI:
10.1002/cphc.200300936

Publication date:
2004

We can see in Figure 5 that the free energy of solvation is linearly related to the shift of the ν_{CO} vibration of acetaminophen for both expanded solvents. This linear behaviour between IR spectroscopic data and the free energy of solvation has been previously reported.[14] This result shows that the ν_{CO} mode is a well-adapted probe to check the acetaminophen solubility sensitivity to CO_2-expanded solvent changes.

To conclude, our results show that high-pressure IR spectroscopy is a valuable tool to investigate, at the molecular-microscopic level, macroscopic phenomena occurring in CO_2-expanded solutions, such as the solubility behaviour of suitable solutes such as **1**.

Acknowledgements

This work was supported by a grant from the contract HPMT-CT-2000 – 00143 between the European Community and the Université de Bordeaux I and also by grants from DGI, Spain (project MAT2003 – 04699) and DGR, Catalunya (project 2001 SGR 00362). Financial support from "Fundación Domingo Martínez" (Spain) and from Catalunya Innovació (CIDEM) is gratefully acknowledged. Santiago Sala is enrolled in the Chemistry Ph.D. Program from the Universitat Autònoma de Barcelona (Spain).

Keywords: acetaminophen · carbon dioxide · IR spectroscopy · solute-solvent interactions · solvent effects

[1] a) E. J. Beckman, *J. Supercrit. Fluids* **2003** (published on the web) DOI: 10.1016/50896-8446(03)00029-9; b) W. Leitner, *Nature* **2003**, *423*, 930; c) L. A. Blanchard, D. Hancu, E. J. Beckman, J. F. Brennecke, *Nature* **1999**, *399*, 28; d) J. M. DeSimone, Z. Guan, C. S. Elsbemd, *Science* **1992**, *257*, 945.

[2] a) P. M. Gallagher, M. P. Coffey, V. J. Krukonis, N. Klasutis, *ACS Symp. Ser.* **1989**, *406*, 334; b) M. Wei, G. T. Musie, D. H. Busch, B. Subramaniam, *J. Am. Chem. Soc.* **2002**, *124*, 2513.

[3] a) N. Ventosa, S. Sala, J. Torres, J. Llibre, J. Veciana, *Crystal Growth & Design* **2001**, *1*, 299; b) P. M. Gallagher, V. Krukonis, G. D. Botsaris, *AIChE Symp. Ser.* **1991**, *87*, 96.

[4] C. A. Eckert, D. Bush, J. S. Brown, C. L. Liotta, *Ind. Eng. Chem. Res.* **2000**, *39*, 4615.

[5] a) J. C. De la Fuente Badilla, C. J. Peters, J. de Swaan Arons, *J. Supercrit. Fluids* **2000**, *17*, 13; b) F. W. Giacobbe, *Fluid Phase Equilib.* **1992**, *72*, 277; c) X. Zhang, B. Han, Z. Hou, J. Zhang, Z. Liu, T. Jiang, J. He, H. Li, *Chem. Eur. J.* **2002**, *8*, 5107.

[6] *The Merck Index*, 12th ed, (Ed.: S. Budavari), Merck & Co. Inc., Whitehouse Station, New Jersey, **1996**, p. 9.

[7] a) M. Poliakoff, S. M. Howdle, S. G. Kazarian, *Angew. Chem.* **1995**, *107*, 1409; *Angew. Chem. Int. Ed.* **1995**, *34*, 1275; b) S. G. Kazarian, M. F. Vincent, F. V. Bright, C. L. Liotta, C. A. Eckert, *J. Am. Chem. Soc.* **1996**, *118*, 1729; c) S. Akimoto, O. Kajimoto, *Chem. Phys. Lett.* **1993**, *209*, 263.

[8] a) T. Tassaing, P. Lalanne, S. Rey, F. Cansell, M. Besnard, *Ind. Eng. Chem. Res.* **2000**, *39*, 4470; b) S. G. Kazarian, R. B. Gupta, M. J. Clarke, K. P. Johnston, M. Poliakoff, *J. Am. Chem. Soc.* **1993**, *115*, 11099; c) Y. Iwai, D. Tanabe, M. Yamamoto, T. Nakajima, M. Uno, Y. Arai, *Fluid Phase Equilib.* **2002**, *193*, 203.

[9] F. E. Wubbolts, Ph. D. Thesis, University of Delft (Netherlands), **2000**.

[10] a) M. Yamamoto, Y. Iwai, T. Nakajima, Y. Arai, *J. Phys. Chem. A* **1999**, *103*, 3525; b) M. A. Blatchford, P. Raveendran, S. L. Wallen, *J. Am. Chem. Soc.* **2002**, *124*, 14818.

[11] $\Delta\tilde{\nu}_{CO}$ corresponds to $\tilde{\nu}_{CO}(X_{CO_2}) - \tilde{\nu}(X_{CO_2} = 0)$.

[12] The cybotactic region is the zone around the solute where the structural order of the solvent molecules has been influenced by the solute: C. R. Yonker, J. C. Linehan, J. L. Fulton in *Chemical Synthesis Using Supercritical Fluids*, chapter 3, (Eds.: P. G. Jessop, W. Leitner), Wiley-VCH, Weinheim, **1999**, p. 195.

[13] J. F. Brennecke, J. E. Chateauneuf, *Chem. Rev.* **1999**, *99*, 433.

[14] a) P. R. Wells, *Linear Free-Energy Relationships.* Academic Press, London, **1968**; b) C. Reichardt, *Solvent Effects in Organic Chemistry*, Verlag Chemie, Weinheim, **1979**.

Received: July 25, 2003 [Z921]

Modelling of the Adsorption of C_{60} on the Au(110) Surface

Richard J. Baxter,[a, b] Petra Rudolf,[c] Gilberto Teobaldi,[a] and Francesco Zerbetto*[a]

The adsorption of organic molecules on inorganic surfaces is a thriving field with applications that range from adhesion, lubrication and chromatographic separation to the modification of the properties of plasticized polymeric materials (e.g., varying the surface and interior concentration of reinforcing fillers), and even to the biocompatibility of artificial internal organs.

Gold surfaces are a prime example of "well-behaved" inorganic surfaces because their reactivity and reconstruction patterns are usually well-understood. While the Au(111) surface is the most studied and exploited because of its high stability, probably second is the more reactive Au(110), which reconstructs into a (1×2) missing row motif, in which alternate rows of atoms along $[1\bar{1}0]$ are removed to produce stable (111) microfacets with 8.16 Å periodicity and 1.4 Å height.[1] In recent years, C_{60} has become one of the most investigated molecules both because of its highly symmetrical shape and because of its properties, foremost among them its electron-accepting capacity. The interaction of C_{60} with gold surfaces has attracted much interest and the structural properties of the C_{60}/metal interface have been studied for Au(111),[2] Au(110),[3] Au(001),[4] and also for polycrystalline Au substrates.[5] The Au(110) missing row (1×2) reconstructed surface provides a corrugated surface, which places more stringent geometric constraints than Au(111) on the

[a] *Dr. R. J. Baxter, Dr. G. Teobaldi, Prof. F. Zerbetto*
Dipartimento di Chimica "G. Ciamician"
Università di Bologna
Via F. Selmi 2, 40126 Bologna (Italy)
Fax: (+39) 051 – 2099456
E-mail: gatto@ciam.unibo.it

[b] *Dr. R. J. Baxter*
Department of Materials, University of Oxford
Parks Road, Oxford, OX1 3PH (UK)

[c] *Prof. P. Rudolf*
Materials Science Centre, University of Groningen
Nijenborgh 4, 9747 AG Groningen (The Netherlands)

 DOI: 10.1002/cphc.200300936

formation of the C_{60} overlayer. The lower surface stability also makes it more versatile, and two entirely independent patterns were observed.[3b, 3c] Gimzewski and co-workers[3b] showed that C_{60} adsorption induces a (1×5) interfacial reconstruction, in which the maximum number of C_{60} molecules bonded to the (110) surface is reached through the formation of a distorted (6×5) overlayer. Pedio et al.[3c] found a more complex C_{60} – Au interface with a large number of Au surface atoms displaced from the original position to form calyxes or cups that accommodate the fullerenes.

The existence of the two interfacial patterns poses the fundamental question of their relative stability and provides a crucial test for any theory of adsorption that requires the careful balance of C_{60} – C_{60} van der Waals interactions with the C_{60} – Au ionic binding and the Au metal state (on this surface the charge of C_{60} has been evaluated as -1 ± 1).[6]

The model used is the same as the one we employed to investigate the adsorption of alkanes and 1-alkenes on Au(111)[7] (other applications of the present model can be found in ref. [8]. The adsorption energies of ten short chains, up to decane and 1-decene, were reproduced with an average error of less than 1 kcal mol^{-1}. In that work, we also studied the unexpected transition to disorder that occurs for the deposition of chains between 18 and 26 carbon atoms, and found that the mismatch between the Au(111) lattice and the CH_2 group periodicity hinders the formation of short, that is, docking, C – Au distances, an event that does not take place for shorter and longer chains.

Table 1 shows a summary of the details of the calculations, including the number of C_{60} molecules and gold atoms in the simulation cells and the axis lengths. The large *c* axis value is necessary to create a gap for the surface. For C_{60}/Au(110), the structure proposed by Gimzewski et al.[3b] has six Au atoms more than the structure proposed by Pedio et al.[3c] Both of them contain four C_{60} molecules in the simulation cell. Because of the different number of Au and C atoms that are present in the cells, a direct comparison of the results is not possible and some care must be exerted. Figure 1 compares the gold overlayers of refs. [3b] and [3c] before and after geometry optimization. The initial, ideal surfaces are obtained simply by mechanical removal of gold atoms. In both cases, the final structures appear smoother (less rough) to the eye. The calyx structure also displays a tendency to disorder, which is caused by the presence of six Au atoms in the topmost layer that are characterized by low coordination numbers, that is, few neighbors.

Table 1 also gives a summary of the energies of the C_{60}/Au cells. Comparison between the energies of the two C_{60}/Au(110) structures shows that the cell of ref. [3b] is more stable. In fact, even assuming that the six Au atoms missing in the second structure have the

Table 1. *Summary of calculation details. Energies [kcal mol^{-1}].[a] The values per Au atom or C_{60} molecule are given in brackets.*

	Structure of ref. [3b]	Structure of ref. [3c]
Nr. of C_{60} molecules per cell	4	4
Nr. of Au atoms per cell	204	198
Nr. of Au layers per cell	8	8
a [Å]	17.31	17.31
b [Å]	20.40	20.40
c [Å]	50.	50.
V_{tot}	−14399.0	−13847.9
$V_{binding} = V_{tot} - V_{Au(relax.)} - V_{C_{60}(relax.)}$	−116.4	−287.6
$V_{int} = V_{tot} - V_{Au} - V_{C_{60}}$	−182.6	−283.1
V_{Au}	−15623.3 (−76.6)	−14988.5 (−75.7)
$V_{C_{60}}$	1406.8 (351.7)	1423.7 (355.9)
$< V >_{100\,K}$	−14251.8	−13736.9
$< V >_{300\,K}$	−13988.4	−13473.5

[a] For Au(110) the cell energy is −18681.0 kcal mol^{-1}; for Au(110) – p(1×2) the cell energy is −21040.6 kcal mol^{-1}; $V_{Au(bulk)} = -87.24$ kcal mol^{-1} (3.78 eV) per atom.

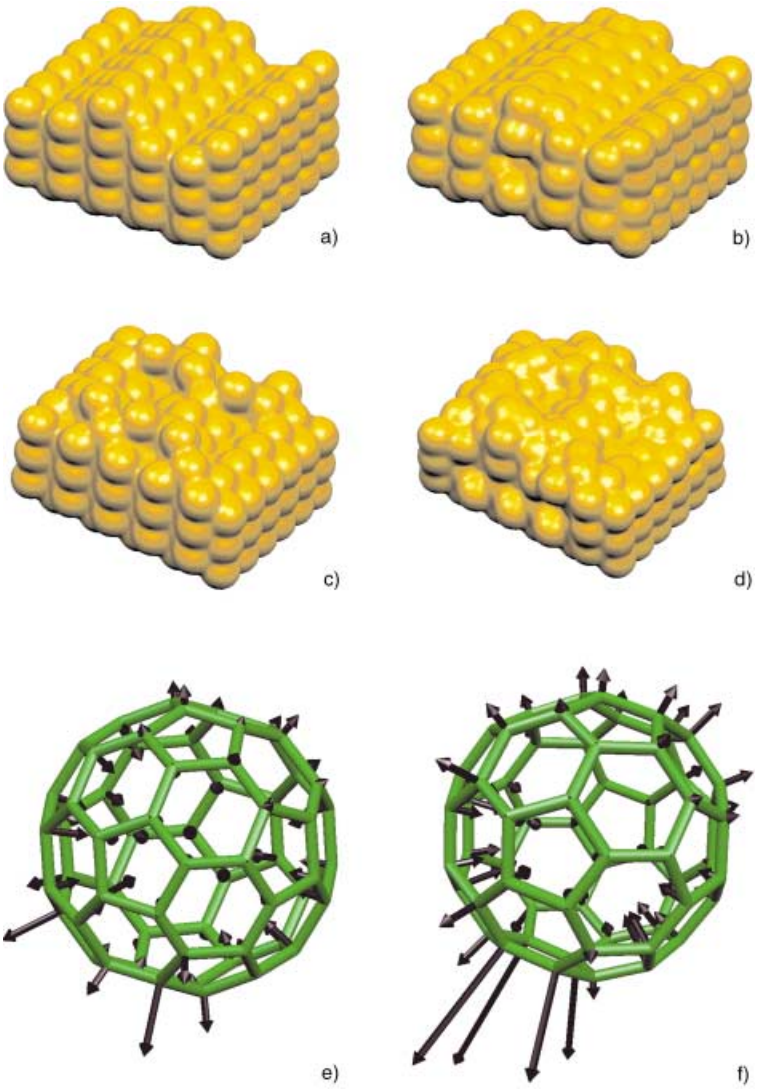

Figure 1. *a) The idealized gold overlayer of the structure of ref. [3b], b) the optimized gold overlayer of the structure of ref. [3b], c) the idealized gold overlayer of the structure of ref. [3c], d) the optimized gold overlayer of the structure of ref. [3c], e) C_{60} on Au(110) following ref. [3b] at 300 K; the tips of the arrows indicate the location of the atoms in the ideal icosahedral configuration (the size of the arrows is multiplied by a factor of 10 to assist the eye); f) C_{60} on Au(110) following ref. [3c] at 300 K; arrows as in (e).*

energy of the bulk, that is, the maximum stability, the cell proposed by Gimzewski et al.[3b] is 27.7 kcal mol^{-1} lower in energy. Interestingly, however, both the interaction and the binding energies (see ref. [9] for a detailed definition) of the interface of the cell of Pedio et al.[3c] are much larger than that for the structure of ref. [3b]. The gold and the C_{60} arrangements energetically penalize the calyxlike structure. If the growth conditions favor metal–molecule interactions, for instance when free Au atoms stick to C_{60} rather than to each other, the structure of Pedio et al. could become important.

To assess the effect of temperature on the structures, we ran molecular dynamics (MD) simulations. Table 1 displays the average energy at 100 and at 300 K. Each average is an enthalpy rather than a free energy, and entropic contributions are not obtained. While the differences of the number of atoms in the cells persist and still make direct comparison difficult, one can notice that at 0 K, that is for the optimized geometry, the energy difference, ΔV, between the two structures is 551.1 kcal mol^{-1}, while both at 100 and 300 K, $\Delta V = 514.9$ kcal mol^{-1}. The energy difference has decreased by 36.2 kcal mol^{-1}! This amount is more than the energy difference that one can estimate at 0 K between the two unit cells, and brings Gimzewski's and Pedio's structures into direct competition. Additionally, the structure of Pedio et al. is more disordered, a property that favors it entropically.

The model also provides the amount of charge transfer from the Au surface to the C_{60} molecules and the relevant gold–carbon distances. Table 2 gives the charges of the individual cages at 0 K and their variations obtained from the MD calculations at 100 and 300 K. The fullerene charge is higher for the structure of Pedio et al. than for the other structure. This is in agreement with the calyx conformation of gold atoms around the molecule and their greater interactions. An increase in the temperature diminishes the average charge on the cages, although in both of the (110) structures one of the fullerenes has a higher charge at 300 K than at 0 K. This higher charge agrees with the parallel decrease in the average distance between the center of mass of C_{60} and the closest Au atom that are given in Table 3 and Table 4. The amount of charge transfer is below one atomic unit (1 electron), in agreement with that deduced from the vibrational spectra of this interface.[6] It is also consistent with a charge transfer lower than $1.0 + 0.2$ atomic units, deduced from the comparison of valence band photoemission intensity near the Fermi edge of C_{60} on Au(110)[10] and C_{60} on polycrystalline Au.[11] The increased width observed for the C1s photo-

Table 2. *Average charges, Q, of the individual C_{60} molecules inside the cells.*

Structure	Molecule	0 K (Opt. geom.)	100 K	300 K
ref. [3b]	$C_{60}(1)$	−0.232	−0.229	−0.225
	$C_{60}(2)$	−0.241	−0.241	−0.221
	$C_{60}(3)$	−0.281	−0.321	−0.315
	$C_{60}(4)$	−0.337	−0.304	−0.270
ref. [3c]	$C_{60}(1)$	−0.417	−0.396	−0.346
	$C_{60}(2)$	−0.353	−0.353	−0.338
	$C_{60}(3)$	−0.355	−0.348	−0.421
	$C_{60}(4)$	−0.400	−0.391	−0.291

Table 3. *Shortest distance from Au atoms to the C_{60} center of mass, Å, and two shortest C-Au distances, R_1 and R_2, Å, for every fullerene of the cell numbered from 1 to 4. The numbers separated by a slash refer to the optimized geometry, the variation of the distance with respect to the average value of the molecular dynamics run at 100 K and the variation of the distance with respect to the molecular dynamics run at 300 K. Positive values indicate elongation of the distance.*

Structure from ref. [3b]	R_{CM}	R_1[a]	R_2[a]
$C_{60}(1)$	5.471/0.067/0.075	2.444/−0.036/−0.108	2.498/−0.018/0.022
$C_{60}(2)$	5.456/0.019/0.111	2.370/0.042/−0.035	2.389/0.101/0.086
$C_{60}(3)$	5.068/−0.240/−0.231	2.346/0.009/−0.057	2.475/−0.038/−0.044
$C_{60}(4)$	4.743/0.180/0.429	2.311/0.029/−0.082	2.340/0.092/0.103
Structure from ref. [3c]	R_{CM}	R_1[a]	R_2[a]
$C_{60}(1)$	4.410/0.087/0.333	2.238/0.099/0.054	2.524/−0.084/-0.098
$C_{60}(2)$	4.715/−0.002/0.024	2.321/0.049/−0.030	2.344/0.100/0.074
$C_{60}(3)$	4.713/0.034/−0.405	2.350/0.005/−0.050	2.351/0.088/0.061
$C_{60}(4)$	4.481/0.043/0.605	2.358/−0.004/−0.068	2.399/0.094/0.023

[a] In the average over the MD trajectory, the atoms with shortest or second shortest distance may vary.

Table 4. *Atomic charges, Q, for the optimized geometry and their variations with respect to the average values of the molecular dynamics runs at 100 K and 300 K. The carbon and the gold atoms are the same whose C-Au distances, R_1 and R_2, are given. Positive values indicate decrease of the electronic charge.*

Structure from ref. [3b]	$Q_{carbon}(R_1)$	$Q_{carbon}(R_2)$	$Q_{gold}(R_1)$	$Q_{gold}(R_2)$
$C_{60}(1)$	−0.018/0.002/0.002	−0.018/0.001/0.001	0.062/0.000/−0.003	0.072/−0.010/−0.013
$C_{60}(2)$	−0.018/0.001/0.002	−0.015/−0.002/−0.002	0.062/−0.001/−0.003	0.062/−0.001/−0.003
$C_{60}(3)$	−0.017/0.001/0.003	−0.017/0.000/0.001	0.052/0.008/0.004	0.083/−0.023/−0.027
$C_{60}(4)$	−0.017/0.001/0.002	−0.017/0.000/0.001	0.052/0.009/0.009	0.044/0.037/0.017
Structure from ref. [3c]	$Q_{carbon}(R_1)$	$Q_{carbon}(R_2)$	$Q_{gold}(R_1)$	$Q_{gold}(R_2)$
$C_{60}(1)$	−0.015/−0.002/0.000	−0.020/0.001/0.003	0.040/0.018/0.009	0.069/−0.015/−0.020
$C_{60}(2)$	−0.011/−0.003/−0.003	−0.012/−0.002/0.004	0.078/−0.016/−0.015	0.078/−0.016/−0.025
$C_{60}(3)$	−0.012/−0.002/−0.002	−0.011/−0.003/−0.004	0.076/−0.008/−0.020	0.076/−0.008/−0.020
$C_{60}(4)$	−0.016/−0.001/0.000	−0.021/0.003/0.004	0.038/0.009/0.012	0.029/0.020/0.021

emission line of C_{60} on Au(110),[10] which was explained as being due to different sites, agrees well with the existence of differently charged cages found here.

C_{60} adsorption also affects its symmetry. In Figures 1e and 1f, the tip of the arrows indicate the average location of the ideal icosahedral structure while the atoms occupy an average position during the MD run at 300 K (the displacement is multiplied by a factor of ten). The direct consequence of the symmetry reduction and of the presence of atoms with different charges is the prediction of the activation in the vibrational spectra of C_{60} on Au of lines that are "silent" in the crystal of the molecule, a feature observed experimentally.[12]

Computational Methods

The molecular force field: We decided to adopt the MM3[13] force field because of the previous experience in our laboratory with this model.[14]

The glue model: The gold surface and its bulk are simulated by the glue model,[15] which contains a density-dependent many-body term in addition to the usual two-body interactions. The former mimics the "gluing" character of the cohesion due to the conduction electrons in metals, where the exact position of neighboring ions is "relatively" unimportant. The potential has a short-ranged "density function" attached to the atoms, so that for each atom in the system one calculates an effective coordination, given by the sum of the density contributions of neighboring atoms. The energy of an atom then depends nonlinearly on this effective coordination.

Organic–Au interactions: The interactions between the metal surface and the molecules are the sum of long-distance and short-distance terms. Here the long-distance part of the potential is taken to scale with the inverse of the distance and is actually of the Coulombic type. The short-distance term is a higher power of the inverse of the distance. The charges are obtained by the charge equilibration (Q_{eq}) scheme of Rappe and Goddard.[16]

A short-range potential is necessary to tune the long-distance one, to account for higher-order terms, and to avoid nuclear fusion when charges or dipoles interact attractively. The choice here was for the Born–Mayer potential[17] because its parameters may be obtained in a general way, although their tuning is usually required (see ref. [7] for more details).

The Q_{eq} scheme, the glue model and the Born Mayer potentials were implemented in the TINKER program,[18] which has been widely used in our lab[14] and implements periodic boundary conditions (PBC). Ewald summation of charges was used both for gold and the adsorbed molecules. Geometries were optimized to root-mean-square (RMS) errors in the gradient smaller than 0.1 kcal mol^{-1} Å^{-1}, and molecular dynamics simulations were run with 20 ps equilibration and at least 100 ps of production.

Acknowledgements

This work was partly supported by EU projects MechMol, IST-2001–35504, and CassiusClays, HPRN-CT-2002–00178, F.Z. and G.T. also acknowledge the contribution of the MURST FIRB program.

Keywords: adsorption · fullerenes · gold · molecular dynamics · surfaces

[1] J. K. Gimzewski, R. Berndt, R. R. Schlittler, *Phys. Rev. B* **1992**, *45*, 6844, and references therein.
[2] a) R. J. Wilson, G. Meijer, D. S. Bethune, R. D. Johnson, D. D. Chambliss, M. S. Devries, H. E. Hunziker, H. R. Wendt, *Nature* **1990**, *348*, 621; b) E. I. Altman, R. J. Colton, *Surf. Science* **1992**, *279*, 49; J. I. Rogero, J. I. Pascual, J. Gomez-Herrero, A. M. Baró, *J. Chem. Phys.* **2002**, *116*, 832.
[3] a) Y. Zhang, X. P. Gao, M. J. Weaver, *J. Phys. Chem.* **1992**, *96*, 510; b) J. K. Gimzewski, S. Modesti, R. R. Schlittler, *Phys. Rev. Lett.* **1994**, *72*, 1036; c) M. Pedio, R. Felici, X. Torrelles, P. Rudolf, M. Capozi, J. Rius, S. Ferrer, *Phys. Rev. Lett.* **2000**, *85*, 1040.
[4] Y. Kuk, D. K. Kim, Y. D. Suh, K. H. Park, H. P. Noh, S. J. Oh, S. K. Kim , *Phys. Rev. Lett.* **1993**, *70*, 1948.
[5] J. L. Wragg, J. E. Chamberlain, H. W. White, W. Krätschmer, D. R. Huffman, *Nature* **1990**, *348*, 623.
[6] S. Modesti, S. Cerasari, P. Rudolf, *Phys. Rev. Lett.* **1993**, *71*, 2469.
[7] R. Baxter, G. Teobaldi, F. Zerbetto, *Langmuir* **2003**, *19*, 7335.
[8] a) C. M. Whelan, F. Cecchet, R. Baxter, F. Zerbetto, G. J. Clarkson, D. A. Leigh, P. Rudolf, *J. Phys. Chem. B* **2002**, *106*, 8739; b) M. Montalti, L. Prodi, N. Zaccheroni, R. Baxter, G. Teobaldi, F. Zerbetto, *Langmuir* **2003**, *19*, 5172.
[9] For binding energy, we take the difference of energies with respect to the relaxed, that is, optimized, isolated fragments. For interaction energy, we take the energy difference of the fragments inside the C_{60}/Au cells, see Table 1.
[10] A. J. Maxwell, P. A. Brühwiler, A. Nilsson, N. Mårtensson, P. Rudolf, *Phys. Rev. B* **1994**, *49*, 10717.
[11] B. W. Hoogenboom, R. Hesper, L. H. Tjeng, G. A. Sawatzky, *Phys. Rev. B* **1998**, *57*, 11939.
[12] P. Rudolf, R. Raval, P. Dumas, G. P. Williams, *Applied Physics A* **2002**, *75*, 147, and references therein.
[13] N. L. Allinger, Y. H. Yuh, J.-H. Lii, *J. Am. Chem. Soc.* **1989**, *111*, 8551.
[14] S. León, D. A. Leigh, F. Zerbetto, *Chemistry, A Eur. J.* **2002**, *8*, 4854; b) G. Bottari, R. Caciuffo, M. Fanti, D. A. Leigh, S. F. Parker, F. Zerbetto, *ChemPhysChem* **2002**, *3*, 1038; c) G. Teobaldi, F. Zerbetto, *J. Am. Chem. Soc.* **2003**, *125*, 7388.
[15] F. Ercolessi, M. Parrinello, E. Tosatti, *Philos. Mag. A* **1988**, *58*, 213.
[16] A. K. Rappe, W. A. Goddard III, *J. Phys. Chem.* **1991**, *95*, 3358.
[17] M. Von Born, J. E. Mayer, *Zeitschrift für Physik* **1933**, *75*, 1.
[18] a) J. W. Ponder, F. J. Richards, *J. Comput. Chem.* **1987**, *8*, 1016; b) C. Kundrot, J. W. Ponder, F. J. Richards, *J. Comput. Chem.* **1991**, *12*, 402; c) M. J. Dudek, J. W. Ponder, *J. Comput. Chem.* **1995**, *16*, 791.

Received: August 13, 2003 [Z936]

